AD-A184 341 STEADY SHEARING IN A VISCOPLASTIC SOLID(U) ARMY 1/1
BALLISTIC RESEARCH LAB ABERDEEN PROVING GROUND MD
T W WRIGHT JUN 87 BRL-TR-2810

UNCLASSIFIED F/G 20/11 NL

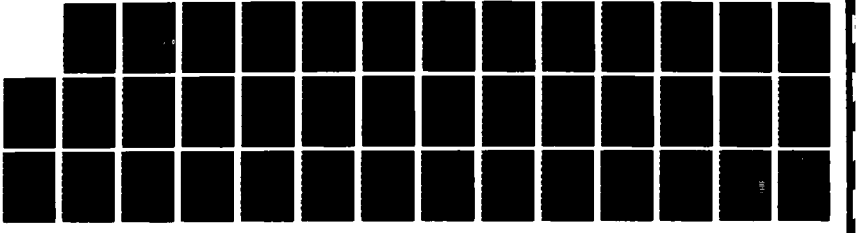

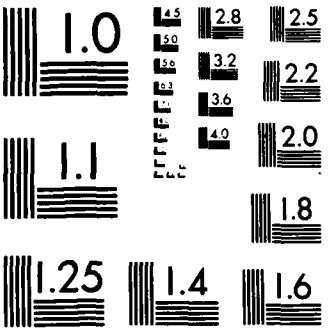

(12)

AD

TECHNICAL REPORT BRL-TR-2810

STEADY SHEARING IN A VISCOPLASTIC SOLID

THOMAS W. WRIGHT

JUNE 1987

US ARMY BALLISTIC RESEARCH LABORATORY
ABERDEEN PROVING GROUND, MARYLAND

DESTRUCTION NOTICE

Destroy by any method that will prevent disclosure of contents or reconstruction of the document.

Additional copies of this report may be obtained from the Defense Technical Information Center, Cameron Station, Alexandria, VA 22314, in accordance with directives in AR 70-31.

The findings in this report are not to be construed as an official Department of the Army position, unless so designated by other authorized documents.

The use of trade names or manufacturers' names in this report does not constitute indorsement of any commercial product.

UNCLASSIFIED
SECURITY CLASSIFICATION OF THIS PAGE

REPORT DOCUMENTATION PAGE

Form Approved
OMB No 0704-0188
Exp Date Jun 30, 1986

1a REPORT SECURITY CLASSIFICATION: Unclassified	1b. RESTRICTIVE MARKINGS
2a SECURITY CLASSIFICATION AUTHORITY	3. DISTRIBUTION / AVAILABILITY OF REPORT: Approved for public release; distribution is unlimited.
2b DECLASSIFICATION / DOWNGRADING SCHEDULE	
4 PERFORMING ORGANIZATION REPORT NUMBER(S)	5. MONITORING ORGANIZATION REPORT NUMBER(S)
6a NAME OF PERFORMING ORGANIZATION: Ballistic Research Laboratory / 6b. OFFICE SYMBOL (If applicable): SLCBR-TB-S	7a. NAME OF MONITORING ORGANIZATION
6c. ADDRESS (City, State, and ZIP Code): Aberdeen Proving Ground, MD 21005-5066	7b. ADDRESS (City, State, and ZIP Code)
8a. NAME OF FUNDING / SPONSORING ORGANIZATION / 8b. OFFICE SYMBOL (If applicable)	9. PROCUREMENT INSTRUMENT IDENTIFICATION NUMBER
8c. ADDRESS (City, State, and ZIP Code)	10. SOURCE OF FUNDING NUMBERS: PROGRAM ELEMENT NO. / PROJECT NO / TASK NO / WORK UNIT ACCESSION NO

11 TITLE (Include Security Classification): Steady Shearing in a Viscoplastic Solid

12 PERSONAL AUTHOR(S): Wright, Thomas W.

13a TYPE OF REPORT	13b TIME COVERED	14 DATE OF REPORT (Year, Month, Day)	15 PAGE COUNT
Technical	FROM _____ TO _____		

16 SUPPLEMENTARY NOTATION

17 COSATI CODES			18 SUBJECT TERMS (Continue on reverse if necessary and identify by block number)
FIELD	GROUP	SUB-GROUP	Adiabatic Shear, Steady Solutions, Viscoplasticity, Boundary Layer
20	11		

19 ABSTRACT (Continue on reverse if necessary and identify by block number)

Steady shearing solutions are found as quadratures within the context of a simple theory of viscoplasticity which includes thermal softening and heat condution. The solutions are illustrated by numerical examples for four commonly used versions of viscoplasticity, where each version has first been calibrated against the same hypothetical data set. It is found that, although they give results that differ in detail, the four flow laws predict qualitatively similar morphology and appear to give rough agreement with physical measurements of adiabatic shear bands. The conjecture is made that steady solutions correspond to central boundary layers for the full unsteady theory.

20 DISTRIBUTION / AVAILABILITY OF ABSTRACT	21 ABSTRACT SECURITY CLASSIFICATION
☐ UNCLASSIFIED/UNLIMITED ☒ SAME AS RPT ☐ DTIC USERS	Unclassified
22a NAME OF RESPONSIBLE INDIVIDUAL: Thomas W. Wright	22b TELEPHONE (Include Area Code): (301) 278-6046 / 22c OFFICE SYMBOL: SLCBR-TB-S

DD FORM 1473, 84 MAR — 83 APR edition may be used until exhausted. All other editions are obsolete.

SECURITY CLASSIFICATION OF THIS PAGE
UNCLASSIFIED

TABLE OF CONTENTS

LIST OF ILLUSTRATIONS

LIST OF TABLES

1. INTRODUCTION

Adiabatic shear bands form during high rate shearing of a solid when thermal softening is stronger than the combined effects of strain hardening and strain rate hardening. In homogeneous shearing, with a constant applied strain rate, the stress rises at first then reaches a maximum at a critical strain where all hardening and softening mechanisms are in balance, and finally begins to fall with increasing strain. Small initial imperfections, that is, small spatial fluctuations in initial temperature, strength, strain rate, and so forth, remain small until the critical strain is passed. Thereafter an imperfection begins to grow, slowly at first, but later at an extremely rapid rate, and as it grows, the deformation tends to concentrate in a narrow band. In the core of the band the temperature and plastic strain rate shoot up during this latter stage while the stress falls precipitously due to rapid thermal softening. In the outer regions the stress also falls rapidly due to momentum transfer from the core, and eventually the outer material returns to an elastic state as the plastic strain rate and plastic working fall to zero. Since there is then no more plastic heating in the outer region, the temperature rise ceases there, and a strong temperature contrast develops between the interior and exterior of the band.

Departure from the unstable homogeneous deformation, as described above, continues to develop with the actively deforming plastic region becoming narrower and narrower and the temperature gradient becoming steeper and steeper, so that if the process is continued long enough, heat conduction becomes a significant factor in removing excess energy from the interior of the band and may provide a limiting mechanism on further growth of the band. Therefore, in the final stages, deformation may proceed in a quasi-steady fashion.

Computations tend to support the preceeding picture of transition from a nearly homogeneous to an extremely inhomogeneous deformation, Wright, Batra[1,2] although the limiting effect of heat conduction has not yet been confirmed by a complete, unsteady calculation that begins with a small perturbation from homogeneous flow and ends with a quasi-steady shear band. Accordingly, it seems worthwhile to examine the full equations of thermo/visco/plasticity in one dimension for the existence of steady solutions, that is, solutions that are independent of time. It turns out that such solutions do exist, and at least for the constitutive equations discussed in this paper, they can be expressed as simple quadratures.

In this paper the general nature of these quadratures is exhibited, and for purposes of comparison, their predictions for four different visco/plastic flow laws are calculated, each law having first been calibrated to agree among themselves under hypothetical conditions of homogeneous, high rate testing.

2. EQUATIONS OF MOTION AND GENERAL SOLUTIONS

A simple version of one dimensional shearing in a visco/plastic material with thermal softening and heat conduction may be expressed as follows.

$$
\begin{aligned}
\rho\dot{v} &= s_{,y} \\
\dot{s} &= \mu(v_{,y} - \dot{\gamma}_p) \\
\rho c\dot{\theta} &= (k\theta_{,y})_{,y} + s\dot{\gamma}_p \\
f(s,\theta,\dot{\gamma}_p) &= \kappa \\
\dot{\kappa} &= M\dot{\gamma}_p
\end{aligned}
\tag{1}
$$

The first equation expresses the balance of linear momentum where s is shear stress, ρ is density, and v is particle velocity in a direction perpendicular to the spatial coordinate y. The comma denotes partial differentiation with respect to y, and the dot denotes partial differentiation with respect to time t. The second equation states that the stress rate is proportional to the elastic strain rate, $\dot{\gamma}_p$ being the plastic strain rate, and μ the elastic shear modulus. The third equation expresses the balance of energy, ignoring thermal expansion and thermoelastic effects, but including heat conduction. The temperature, measured from a convenient reference level, is θ, c is specific heat, and k is thermal conductivity, which may depend on temperature. Plastic work is regarded as being converted completely to heat, so that the rate of plastic work acts as a source in the energy equation. The fourth equation states that yielding is determined by a sequence of surfaces in stress/temperature space with plastic strain rate as a parameter where κ is a measure of work hardening. The last equation is a postulated relation for the evolution of κ where M is a constitutive function that depends on s, θ, and κ.

Equation (1.4) is assumed to apply if $f(s,\theta,0) > \kappa$, and then it is further assumed that (1.4) can be inverted uniquely to give

$$\dot{\gamma}_p = g(s,\theta,\kappa) \tag{2}$$

where g has the same sign as s to ensure that plastic work is always positive, and $g_s > 0$, $g_\theta > 0$, and $g_\kappa < 0$, subscripts denoting differentiation with respect to the argument indicated. If $f(s,\theta,0) \leq \kappa$, then $\dot{\gamma}_p = 0$. This is a fairly general version of viscoplasticity as an overstress phenomenon, which is broad enough to include those in common usage, as described by Malvern[3] for example, including those that do not use a definite yield surface at all. In the latter case, (2) is postulated right from the start. Then there is always some plastic flow, although the plastic strain rate becomes extremely small when the stress falls below some evolving reference level. In a further generalization, the function M, f, and g could depend on γ_p as well. In any case the variables γ_p and κ both have the status of internal variables controlled respectively by (2) and (1.5).

In a steady shearing motion the stress, particle velocity, and temperature depend only on position, but not on time, so that equations (1) become ordinary differential equations. Inspection of equations (1) and (2) reveals that general solutions do not exist unless $\kappa = 0$ throughout the region under consideration, and g does not depend explicitly on γ_p. That is to say, saturation has occurred so that there is no further work hardening and the plastic strain rate is independent of further levels of plastic strain. From (1.4) and the requirement that $g \not\equiv 0$ inside the shear band it follows that $M(s,\theta,\kappa) = 0$. Let it be assumed that this equation can be solved for κ as a function of s and θ, say $\kappa = \hat{\kappa}(s,\theta)$. The steady equations may now be written as follows.

$$\begin{aligned} s_{,y} &= 0 \\ v_{,y} &= g(s,\theta,\kappa) \\ (k\theta_{,y})_{,y} &+ sg(s,\theta,\kappa) = 0 \end{aligned} \tag{3}$$

where $\kappa = \hat{\kappa}(s,\theta)$. Equations (3) have the solution

$$s = \bar{s} = \text{const}$$

$$\tfrac{1}{2}(k\theta_{,y})^2 = \bar{s}\int_{\theta}^{\theta c} k(\theta')\, g(\bar{s},\theta',\hat{\kappa}(s,\theta'))\, d\theta' \tag{4}$$

$$v = \pm\sqrt{\frac{2}{\bar{s}}}\left\{\int_{\theta}^{\theta c} k(\theta')\, g(\bar{s},\theta',\hat{\kappa}(s,\theta'))\, d\theta'\right\}^{\frac{1}{2}} = -\frac{k\theta_{,y}}{\bar{s}}$$

Equation (4.2) may be solved by quadrature to obtain θ as an even function of y, where θ_c is the temperature at $y = 0$, which is the center of the band. Equation (4.3) follows from (3.2) with

$$v = \int g\,\frac{dy}{d\theta}\,d\theta + \text{const}$$

after making use of (4.2), or directly from (3.3) after making use of (3.2) and (4.1). In (4.3) the velocity is measured relative to the center of the band and the $\pm$ sign holds for $\pm y$ so that v is odd in y. A complete solution requires specification of $\bar{s}$ and θ_c, or the equivalent, so in general there is a two parameter family of steady solutions.

3. EXAMPLES

The nature of the solutions given above is best illustrated by considering special cases. Four examples of viscoplastic flow laws, which have been used by various researchers in a discussion of shear bands, and all of which fit into the general framework outlined above, are the Arrhenius law

(eg., see Shawki, et al.[4]), the Bodner-Partom-Merzer law (eg., see Merzer[5]), a simple power law (eg., see Shawki, et al.[4]), and the Litonski law (eg., see Wright and Batra[1,2] or Burns[6]). The steady shearing solutions that result from these four laws may be compared after each has been calibrated against the response characteristics of a hypothetical material. Accordingly, let it be supposed that for a series of standard, high rate, isothermal tests, the properties of a typical high strength steel may be summarized as follows.

Test Temperature:	$\theta = 300^{\circ}$ K
Strain Rate:	$\dot{\gamma}_p = 1000\ s^{-1}$
Flow Stress:	$s = 0.5$ GPa
Stain Rate Sensitivity	$m = 0.02$
Thermal Sensitivity	$p = 0.2$

Where m and p are defined as follows:

$$m = \frac{d(\ln s)}{d(\ln \dot{\gamma}_p)} \quad , \quad p = -\frac{d(\ln s)}{d(\ln \theta)} \tag{5}$$

In all cases considered from here on, both the thermal conductivity k and the strain hardening parameter κ are assumed to be constants for ease of computations.

It is convenient to nondimensionalize the plastic strain rate, temperature, particle velocity, and y-coordinate as follows. Let r, η, u, and ξ be the four nondimensional variables with scale factors $\dot{\Gamma}$, T, U, and Y with a possible shift q in the zero for temperature.

$$\dot{\gamma}_p = \dot{\Gamma} r \ , \quad \theta = T\eta + q \ , \quad v = Uu \ , \quad y = Y\xi$$

Then with a nondimensional flow law

$$r = g(\eta),$$

where $g(\cdot)$ may depend on s/κ or other physical parameters as well, equations (4.2) and (4.3) can be expressed as

$$\eta_\xi^2 = \int_\eta^{\eta_c} g(\eta)\, d\eta, \quad u = \left\{ \int_\eta^{\eta_c} g(\eta) \quad d\eta \right\}^{\frac{1}{2}}, \xi = \int_\eta^{\eta_c} \frac{d\eta}{u} \tag{6}$$

where η_c corresponds to the temperature in the center of the band. The three nondimensional variables r, U, and ξ are now given parametrically through the nondimensional temperature. The scale factors for plastic

strain rate and temperature are to be chosen in a convenient manner, and the scale factors for distance and velocity are chosen as follows

$$Y = \left\{\frac{1}{2}\frac{kT}{\bar{s}\dot{\Gamma}}\right\}^{\frac{1}{2}} \qquad U = \left\{2kT\ \dot{\Gamma}/\bar{s}\right\}^{\frac{1}{2}} \tag{7}$$

Each of the four flow laws will now be considered in turn.

3.1 The Arrhenius Flow Law[4].

Written in the form of (2) this flow law is given by

$$\dot{\gamma}_p = \dot{\Gamma}_o \exp\left\{-\frac{V}{b\theta}\ (\kappa - \bar{s})\right\} \tag{8}$$

where $\dot{\Gamma}_o$ is a limiting strain rate, V is activation volume, and b is activation energy per ^oK. Note that there is no fixed yield surface where plastic flow ceases, and that the plastic strain rate approaches an upper limit of $\dot{\Gamma}_o$ as $\bar{s}$ approaches κ from below or as temperature becomes large. With scale factors for plastic strain rate and temperature chosen to be

$$\dot{\Gamma} = \dot{\Gamma}_o \quad , \quad T = \frac{V\bar{s}}{b}\ \left(\frac{\kappa}{\bar{s}} - 1\right) \tag{9}$$

the flow law takes the nondimensional form

$$r = e^{-\frac{1}{\eta}} \tag{10}$$

To be consistent with the calibrating conditions, it is necessary that

$$\frac{V}{b} - = 3\text{x}10^{-5}\ ^oK\text{-m}^3/\text{Joule}\ , \quad \kappa = 0.6\ \text{GPa}\ , \quad \dot{\Gamma}_o = 2.2026\text{x}10^7\ s^{-1}$$

3.2 The Bodner-Partom-Merzer Law[5].

Again written in the form of (2), this flow law takes the form

$$\dot{\gamma}_p = 2D_o \exp\left\{-\frac{1}{2}\left(\frac{\kappa^2}{3\bar{s}^2}\right)^{\left(\frac{a}{\theta} + b\right)}\right\} \tag{11}$$

where $a > 0$ and $b < 0$ are material constants. There is no fixed yield surface, and for $\sqrt{3}\,\bar{s}$ less than κ (the usual case), as the temperature increases to large values, the plastic strain rate tends to a limiting value of $2D_o e^{-\frac{1}{2}}$. The scale factors for plastic strain rate and temperature are chosen as follows.

$$\dot{\Gamma} = 2D_o \,, \quad T = a \tag{12}$$

The plastic flow law is now given by

$$r = \exp\left\{ -\frac{1}{2} \left(\frac{\kappa^2}{3\bar{s}^2} \right)^{\frac{1}{\eta}} + b \right\} \tag{13}$$

and with b arbitrarily set equal to zero, the calibrating conditions require that

$$m = \frac{\theta}{a} \left(\kappa^2/3\bar{s}^2\right)^{-a/\theta} \quad \text{and} \quad 2p = \ln(\kappa^2/3\bar{s}^2).$$

Thus it follows that

$$\kappa = 1.05777 \text{ GPa}, \quad a = 1653.75\ ^{o}\text{K}, \quad D_o = 4.6618\text{x}10^{4}\ \text{s}^{-1}$$

3.3 The Simple Power Law[4].

This flow law, written in the form of (2), is

$$\dot{\gamma}_p = \dot{\Gamma}_o \left(\frac{\bar{s}}{\kappa} \right)^{\frac{1}{n}} \left(\frac{\theta}{\theta_o} \right)^{\frac{\nu}{n}} \tag{14}$$

and again there is no fixed yield surface. With the obvious choices for scale factors

$$\dot{\Gamma} = \dot{\Gamma}_o \,, \quad T = \theta_o \,, \tag{15}$$

the plastic flow law becomes

$$r = \left(\frac{\bar{s}}{\kappa} \right)^{\frac{1}{n}} \eta^{\frac{\nu}{n}} \tag{16}$$

and the calibrating conditions require that $m = n$ and $p = \nu$. There is no unique choice for the other constants, but the simplest choices are

$$\dot{\Gamma}_o = 10^3\ \text{s}^{-1}\,, \kappa = 0.5 \text{ GPa}\,, \theta_o = 300\ ^{o}\text{K}.$$

3.4 The Litonski Law[126].

In the form of (2) this flow law may be written

$$\dot{\gamma}_p = \frac{1}{b}\left\{\left[\frac{\bar{s}}{\kappa[1 - a(\theta - \theta_o)]}\right]^{\frac{1}{n}} - 1\right\} \quad , \tag{17}$$

and now there is a definite yield point, where plastic flow ceases, given by $\bar{s} = \kappa\{1-a(\theta - \theta_o)\}$. Each of the other three flow laws could of course be modified to include a definite yield point if desired. The scale factors for plastic strain rate and temperature are chosen to be

$$\dot{\Gamma} = (1 + b\dot{\gamma}^c)/b \quad , \quad T = [1 - a(\theta_c - \theta_o)]/a \quad , \tag{18}$$

and in this case $q = \theta_o + [1 - (\bar{s}/\kappa)]/a$. In this equation θ_c and $\dot{\gamma}_p^c$ are the temperature and plastic strain rate in the center of the band, and the factors T and q are obtained from the change of variable $\eta = [a(\theta - \theta_o) + \bar{s}/\kappa - 1]/[1 - a(\theta_c - \theta_o)]$. The plastic flow law in these variables is now given by

$$r = \left[(1 + b\gamma^c)^n - \eta\right]^{\frac{1}{n}} - (1 + b\dot{\gamma}_p^c)^{-1} \tag{19}$$

The calibrating conditions require that

$$m = n\,\frac{b\dot{\gamma}_p}{1 + b\dot{\gamma}_p} \quad , \quad p = \frac{a\theta}{1 - a(\theta - \theta_o)}$$

With θ_o and b arbitrarily chosen to be 300 ^oK and 1000 s^{-1}, then n = m to a close approximation, $a = \frac{2}{3} \times 10^{-3}$ ^oK and $\kappa = 0.37929$ GPa. With the aid of the flow law (17) the scale factors Y and U may be rewritten as

$$Y = \sqrt{\frac{kb}{2a\kappa}}\;(1 + b\dot{\gamma}_p^c)^{-\frac{n+1}{2}} \quad , \quad U = \sqrt{\frac{2k}{\kappa ab}}\;(1 + b\dot{\gamma}_p^c)^{\frac{1-n}{2}}$$

In this form it is clear that solutions depend only weakly on b for large values of b.

In order to compare the four flow laws, the steady shearing solution has been computed for the six cases shown in the Table, where the temperature and strain rate at the center of the band have been fixed as the two defining parameters.

Table 1. Cases Considered

CASE	A	B	C	D	E	F
θ_c	400 ^oK	400 ^oK	400 ^oK	500 ^oK	500 ^oK	600 ^oK
$\dot{\gamma}_p^c$	10^3 s^{-1}	10^4 s^{-1}	$5x10^4$ s^{-1}	10^4 s^{-1}	$5x10^4$ s^{-1}	$5x10^4$ s^{-1}

Except for the Bodner-Partom-Merzer law at the higher strain rates and temperatures, the general configuration of the solutions for the four laws are broadly similar to the curves shown in Figure 1. (The figure actually represents the Litonski law for either case B or D.) Plastic strain rate is highest at the center of the band, but falls rapidly to much smaller values toward the sides where it levels out. Temperature also is highest in the center and falls off toward the sides, but as the plastic strain rate levels off, the temperature gradient tends toward a constant negative value, so that the heat generated by plastic work is just balanced by heat conduction. Particle velocity relative to the center of the band increases rapidly at first and then levels off and approaches a constant value asymptotically.

The figure shows that there is no one definitive width to the band, so for purposes of numerical comparison, the width, denoted d, will be arbitrarily defined as the distance from the center of the band at which the plastic strain rate falls to one tenth of its maximum value. In the figure this distance is shown by the tick mark on each curve. At that distance the temperature gradient and the particle velocity are within a few percent of their asymptotic values. The following six tables compare the widths, temperatures, velocities and stresses for each of the six cases listed in Table 1. The value used for the thermal conductivity is that for a typical steel, $k = 46.7$ J s^{-1} m^{-1} $^oK^{-1}$.

Table 2. Case A: $\theta_c = 400\ ^oK$, $\dot{\gamma}_p^c = 10^3\ s^{-1}$

	Width d, μm	Temperature θ(d), ^oK	Velocity v(d), m/s	Stress s, GPa
Arrhenius	143.7	325	0.079	0.467
B-P-M	129.4	337	0.075	0.468
Power	151.4	317	0.081	0.472
Litonski	137.9	334	0.071	0.467

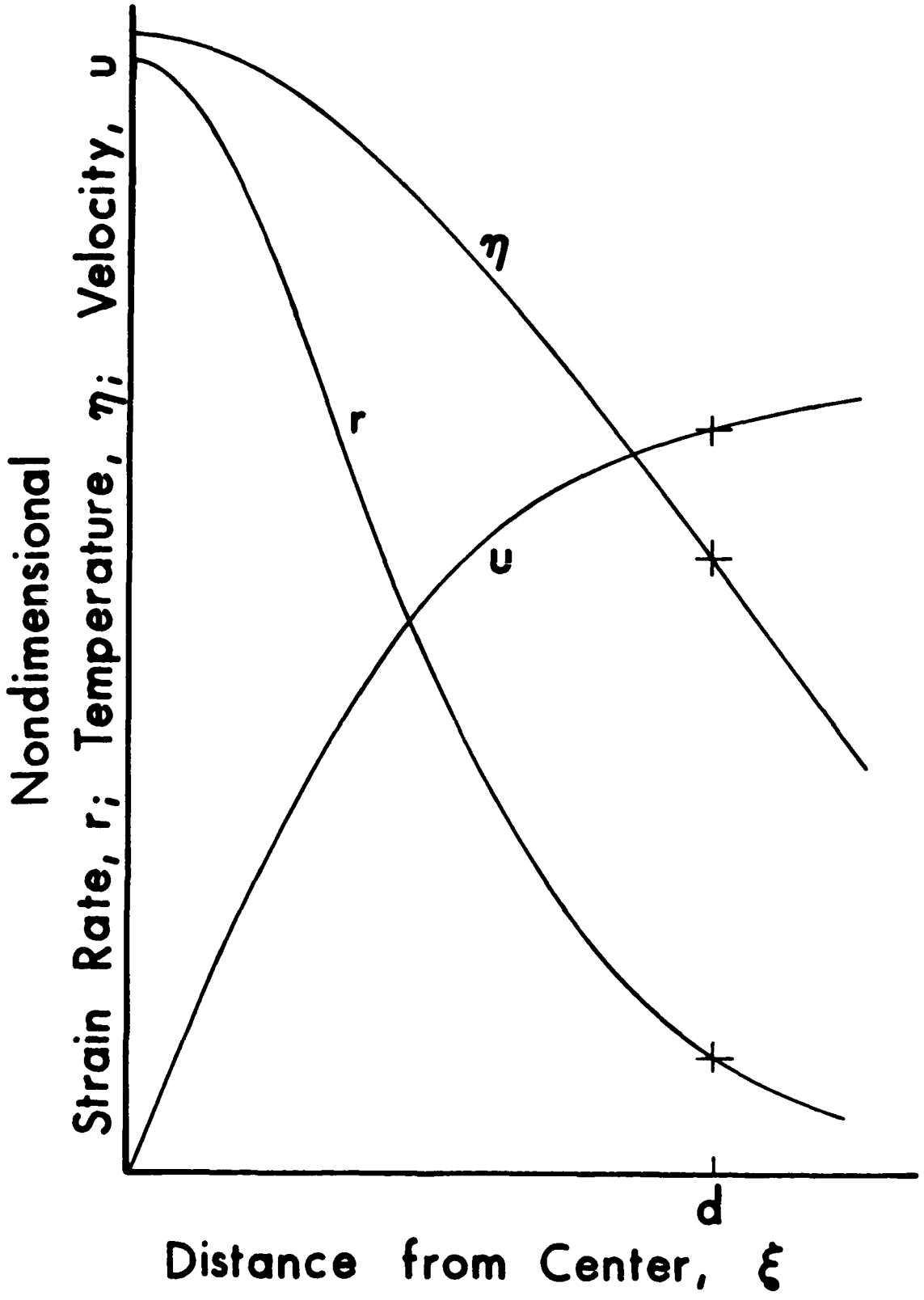

Figure 1. Typical Distribution of Plastic Strain Rate, Temperature, and Velocity vs Distance from the Center of a Shear Band.

Table 3. Case B: $\theta_c = 400\ ^{o}K$, $\dot{\gamma}_p^c = 10^4\ s^{-1}$

	Width d, μm	Temperature θ(d), °K	Velocity v(d), m/s	Stress s, GPa
Arrhenius	48.5	308	0.272	0.497
B-P-M	54.3	271	0.343	0.510
Power	46.8	317	0.251	0.494
Litonski	42.7	334	0.221	0.489

Table 4. Case C: $\theta_c = 400\ ^{o}K$, $\dot{\gamma}_p^c = 5x10^4\ s^{-1}$

	Width d, μm	Temperature θ(d), °K	Velocity v(d), m/s	Stress s, GPa
Arrhenius	23.1	290	0.657	0.519
B-P-M	33.9	48.6	1.486	0.595
Power	20.6	317	0.553	0.510
Litonski	18.8	334	0.487	0.505

Table 5. Case D: $\theta_c = 500\ ^{o}K$, $\dot{\gamma}_p^c = 10^4\ s^{-1}$

	Width d, μm	Temperature θ(d), °K	Velocity v(d), m/s	Stress s, GPa
Arrhenius	55.7	385	0.312	0.472
B-P-M	62.1	339	0.393	0.487
Power	53.4	397	0.288	0.473
Litonski	42.7	439	0.221	0.454

Table 6. Case E: $\theta_c = 500\ ^{o}K$, $\dot{\gamma}_p^c = 5x10^4\ s^{-1}$

	Width d, μm	Temperature θ(d), °K	Velocity v(d), m/s	Stress s, GPa
Arrhenius	26.3	367	0.749	0.499
B-P-M	38.0	56.6	1.666	0.591
Power	23.5	397	0.632	0.488
Litonski	18.8	439	0.487	0.469

Table 7. Case F: $\theta_c = 600\ ^{o}K$, $\dot{\gamma}_p^c = 5x10^4\ s^{-1}$

	Width d, μm	Temperature θ(d), °K	Velocity v(d), m/s	Stress s, GPa
Arrhenius	29.4	435	0.838	0.478
B-P-M	----	---	-----	-----
Power	26.2	476	0.706	0.471
Litonski	18.8	543	0.487	0.433

The values for the Bodner-Partom-Merzer law are not shown for the last case because, as in cases C and E above, the temperature at the edge of the band seems unrealistically low. This seems to be caused by the extreme sensitivity to temperature of this flow law and by the moderately high central strain rate, which is more than half the limiting strain rate. Figure 2 shows the computed profiles for the B-P-M law for case E. Note that the distribution of the higher plastic strain rates is much broader than the distribution shown in Figure 1 and that it plunges much more rapidly. Furthermore, the plastic strain rate does not vanish until the temperature reaches absolute zero.

Figures 3-6 compare the width, edge velocity, driving stress, and edge temperature for all four flow laws with a fixed central temperature of 400 °K and increasing plastic strain rate. The widths all decrease sharply with increasing strain rate, whereas the edge velocity and driving stresses show marked increases. The trend in each case is the same, and the widths even agree fairly well, but the edge velocity and driving stress for the B-P-M law depart sharply from the others at the highest strain rate. Since the temperature gradient in every case becomes steeply negative toward the edge of the band, a comparison of temperatures at the distance d from the center is only a rough, but still useful, measure of the temperature contrast to be found across a shear band. Only the B-P-M law shows a strong effect of increasing strain rate whereas the other three have only a modest temperature drop of 60-110 °K.

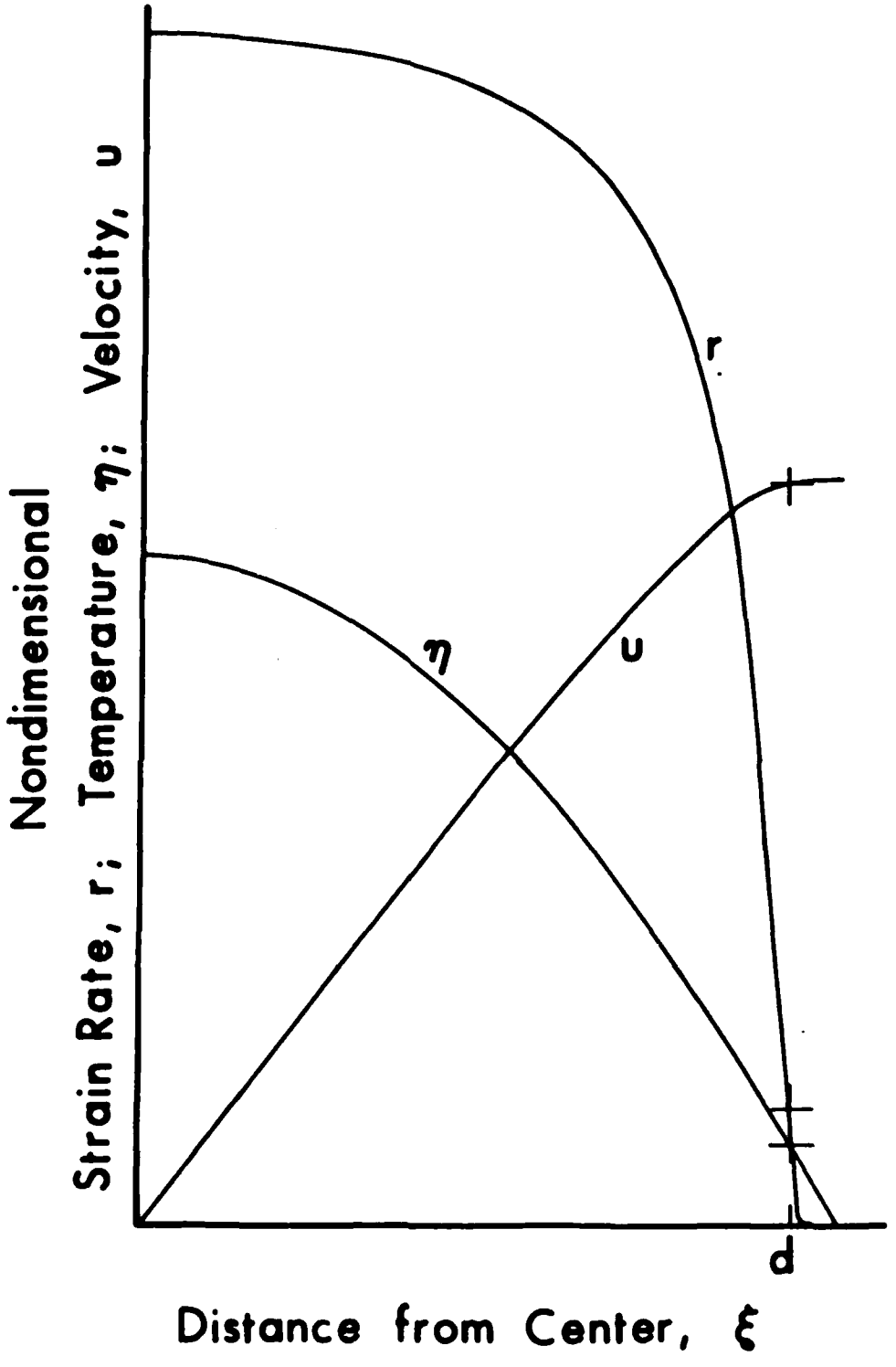

Figure 2. Distribution of Plastic Strain Rate, Temperature, and Velocity vs Distance from the Center of a Shear Band According to the B-P-M Law for a High Central Strain Rate.

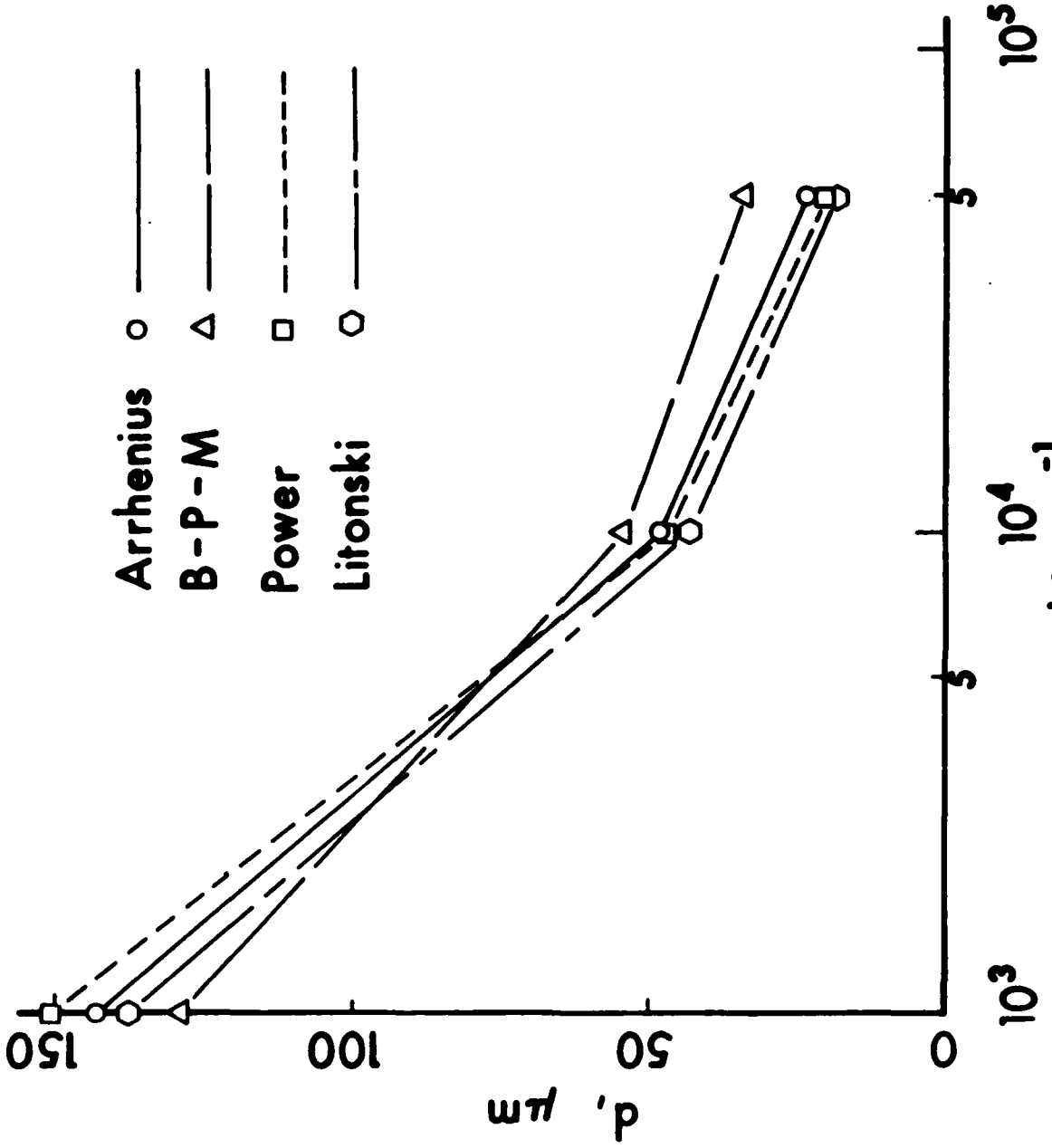

Figure 5. Width vs Central Plastic Strain Rate When the Central Temperature is 400°K.

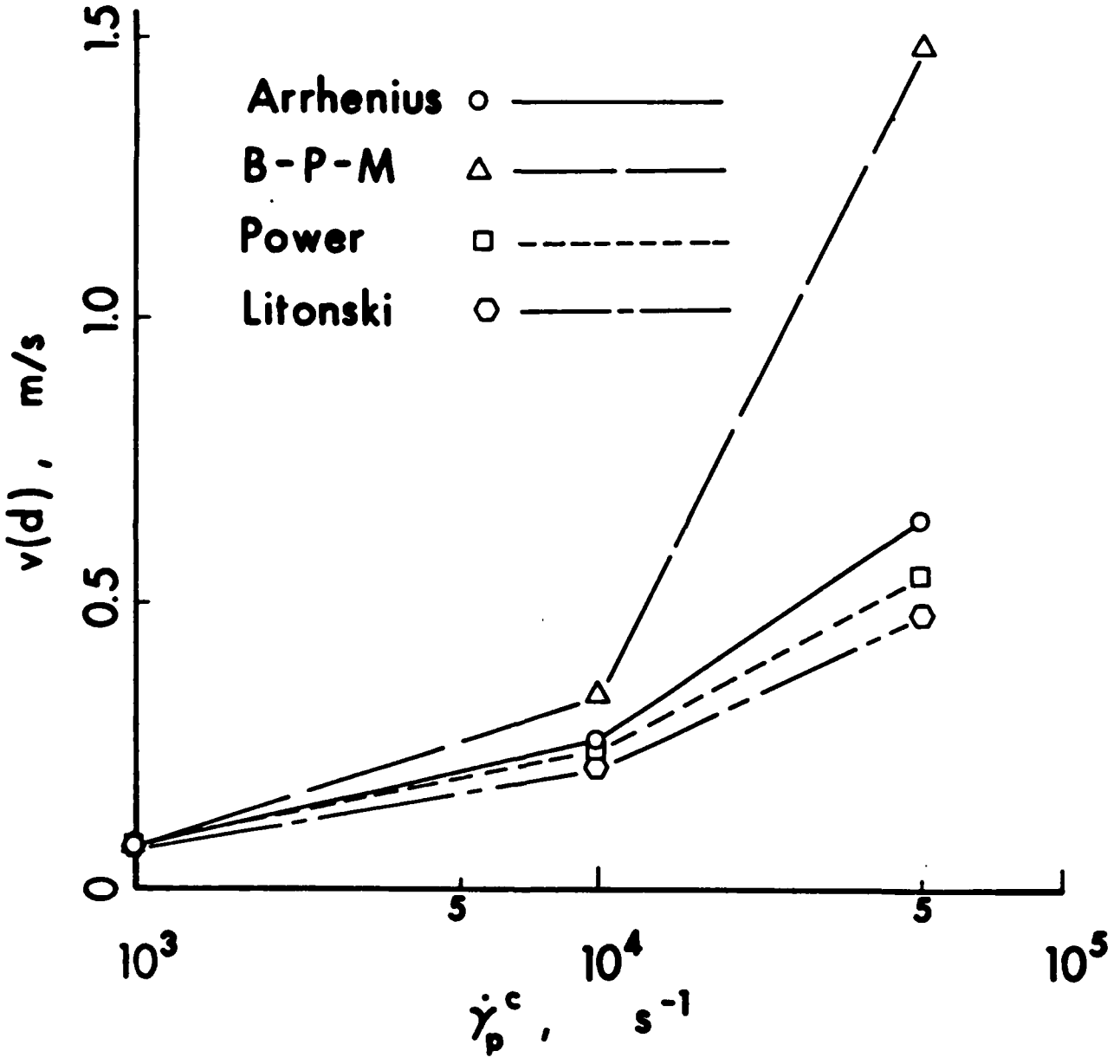

Figure 4. Edge Velocity vs Central Plastic Strain Rate When the Central Temperature is 400°K.

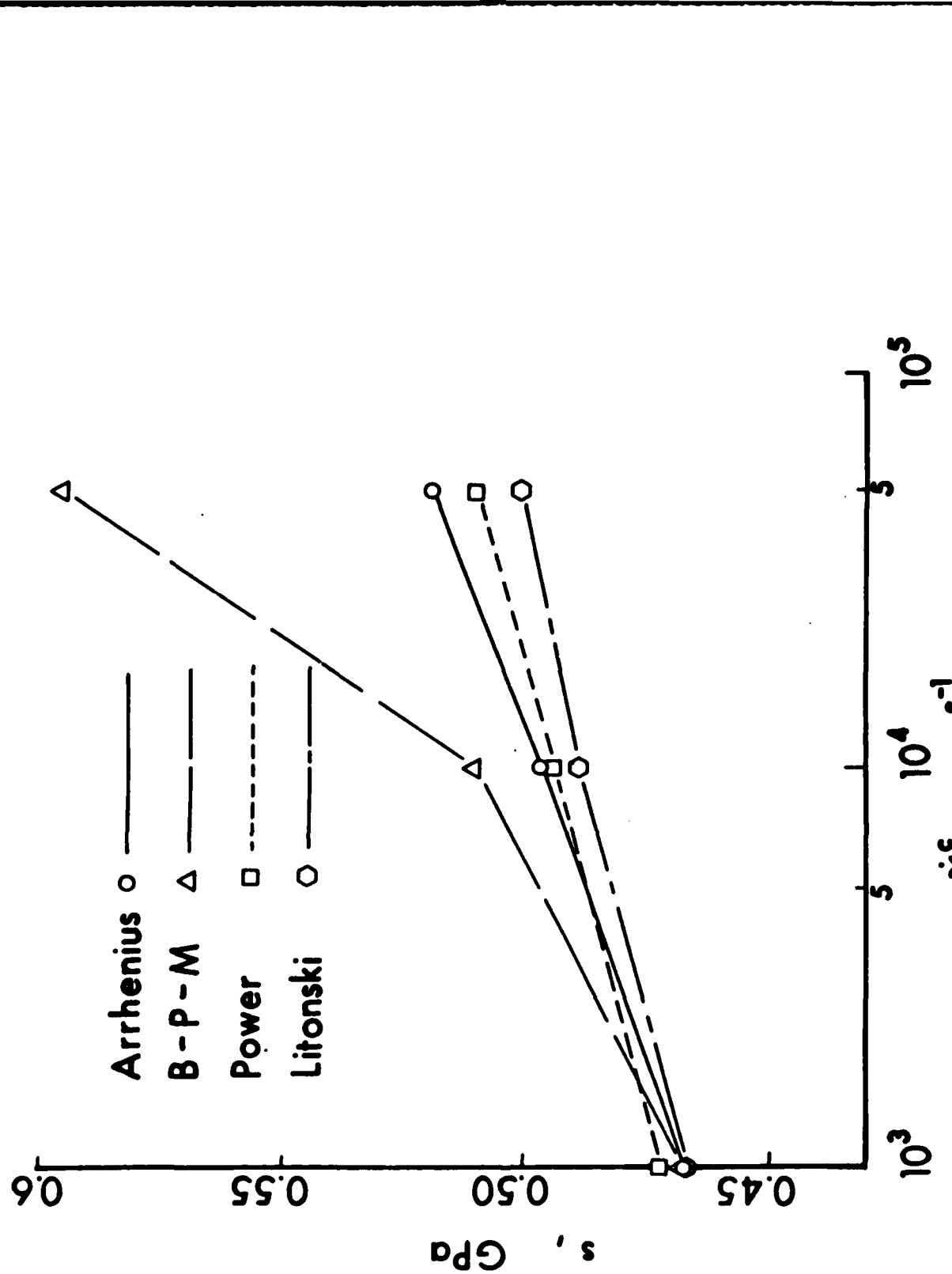

Figure 5. Driving Stress vs Central Plastic Strain Rate When the Central Temperature is 400°K.

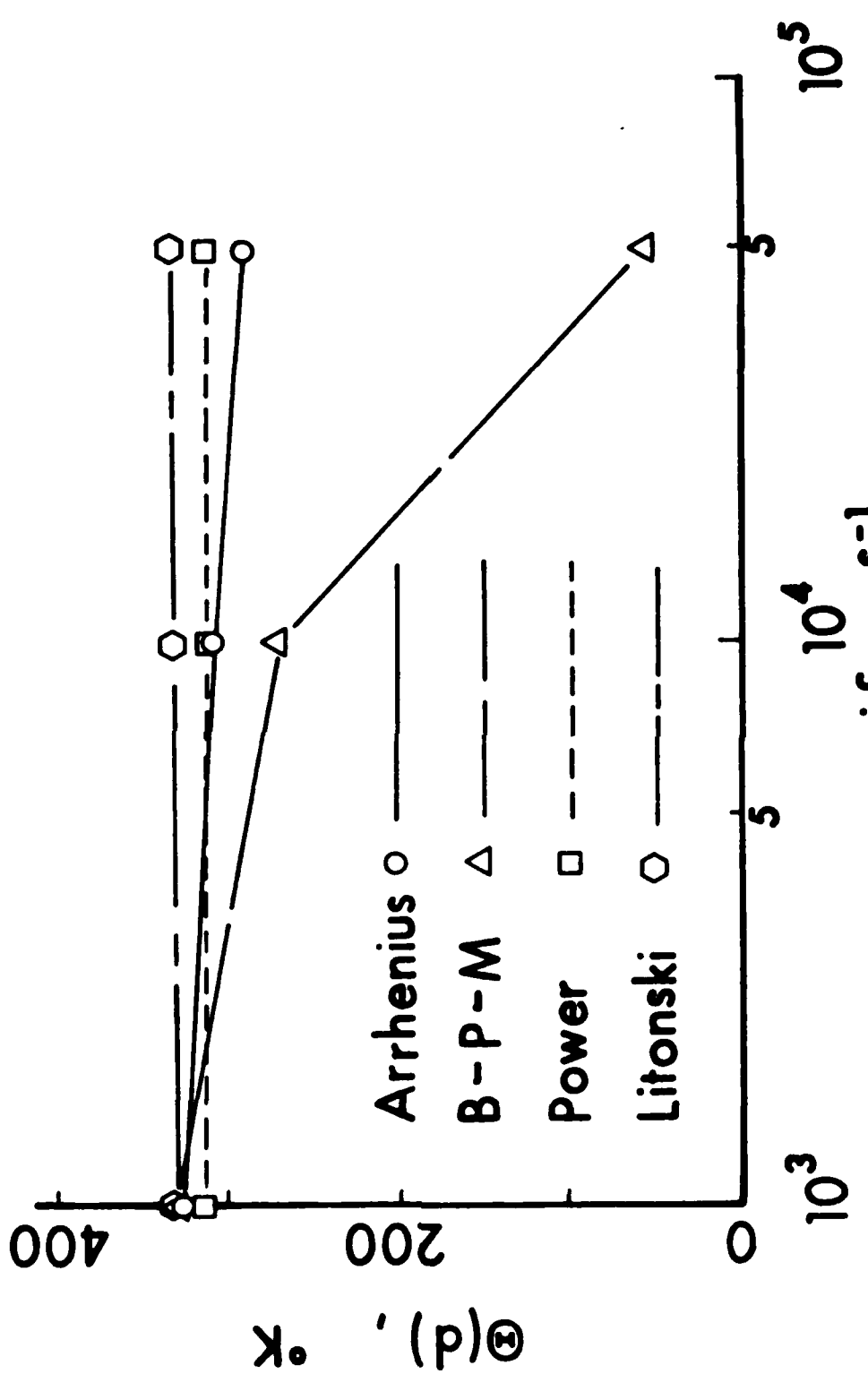

Figure 6. Edge Temperature vs Central Plastic Strain Rate When the Central Temperature is 400°K.

For fixed strain rate, Figures 7-10 show the effect of central temperature on width, edge velocity, driving stress, and temperature contrast. Once again the B-P-M law appears to be significantly different from the other three laws. The width and edge velocity for the Litonski law are independent of temperature, whereas the others show an increase with increasing central temperature, with the B-P-M law lying well above the others. Driving stress decreases with temperature in all cases, with the B-P-M law requiring the highest stresses and showing the least influence of increasing temperature. Temperature contrast from the center of the band to a distance d away from the center shows the most marked differences among the four flow laws. The Litonski law is almost constant with increasing central temperature and shows the least contrast. The Arrhenius and power laws show somewhat greater contrast and increase slightly with increasing temperature, and the B-P-M law shows a very large and strongly temperature dependent temperature contrast.

4. DISCUSSION

Since steady shearing solutions depend on a saturation effect in work hardening and, in their outer regions, tend asymptotically toward finite temperature gradient and particle velocity, as well as constant stress throughout, they cannot give a complete solution if work hardening continues, or if the temperature gradient is required to vanish at the boundary, or if the imposed boundary conditions are truly unsteady.

However, if the parameters that define a steady solution are only slowly varying functions of time, then these solutions may play the role of central boundary layers for more complete dynamic solutions. In fact, when time is scaled according to the rule $t = \tau/\delta$ in the full dynamical equations, then the steady equations result in the limit as $\delta \to 0$. With τ being held fixed $t \to \infty$, so the steady equations apparently have the interpretation of holding asymptotically at large times. In that case the outer morphological characteristics of these steady solutions would be used to derive central boundary conditions for the exterior solution, that is, the solution away from the shear band. This possibility will be explored in a future paper.

Since the rate and temperature conditions to be found in the center of a band differ considerably from the calibrating conditions, it is to be expected that the structure of a real shear band would differ somewhat from that predicted by any particular hypothetical rate law. Thus, it is somewhat surprising that the morphology predicted by the four rate laws in this paper agree as well as they do. Furthermore, although the measure of width d is somewhat arbitrarily chosen, the values calculated for d, based upon physical constants for steel, seem to be of the right order of magnitude according to actual physical measurements on shear bands. For example, Moss[7] shows a photomicrograph and data plots for a shear band in a high strength NiCr steel where the strain rate apparently dropped by an order of magnitude every 10 to 15 microns. No definitive comparison can be made at this time, however.

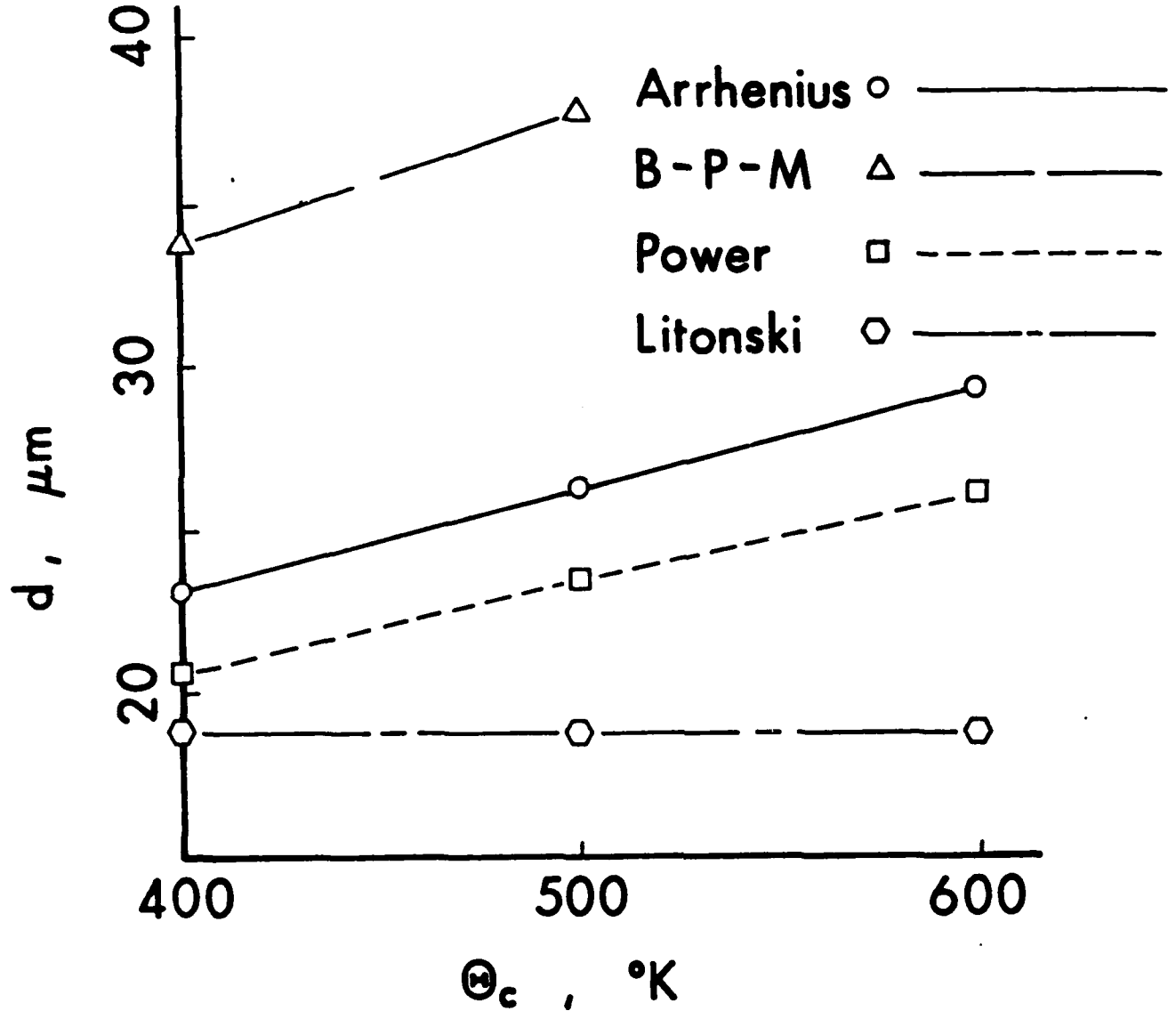

Figure 7. Width vs Central Temperature When the Central Plastic Strain Rate is 5×10^4 s^{-1}.

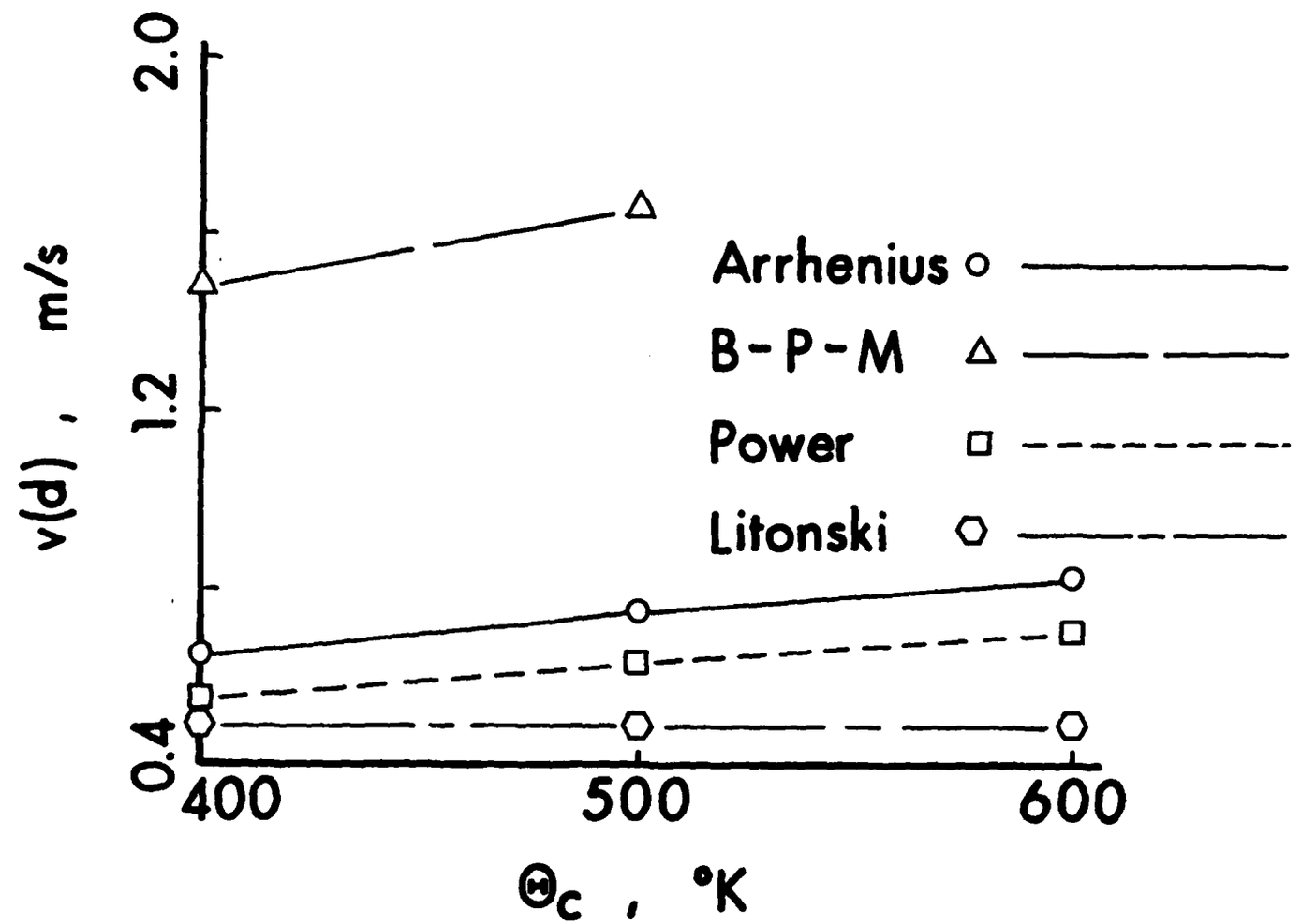

Figure 8. Edge Velocity vs Central Temperature When the Central Plastic Strain Rate is $5 \times 10^4 s^{-1}$.

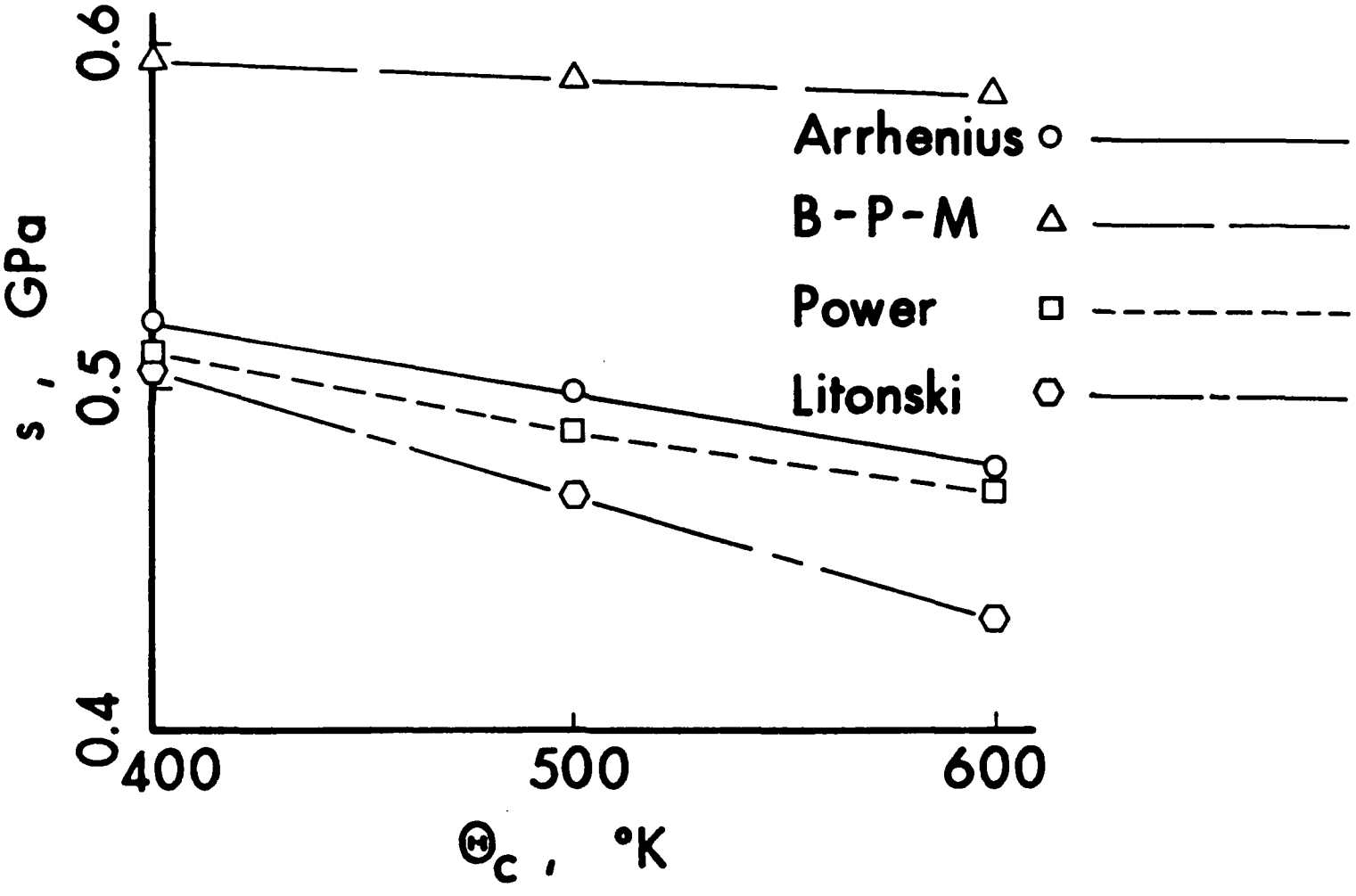

Figure 9. Driving Stress vs Central Temperature When the Central Plastic Strain Rate is 5×10^4 s^{-1}.

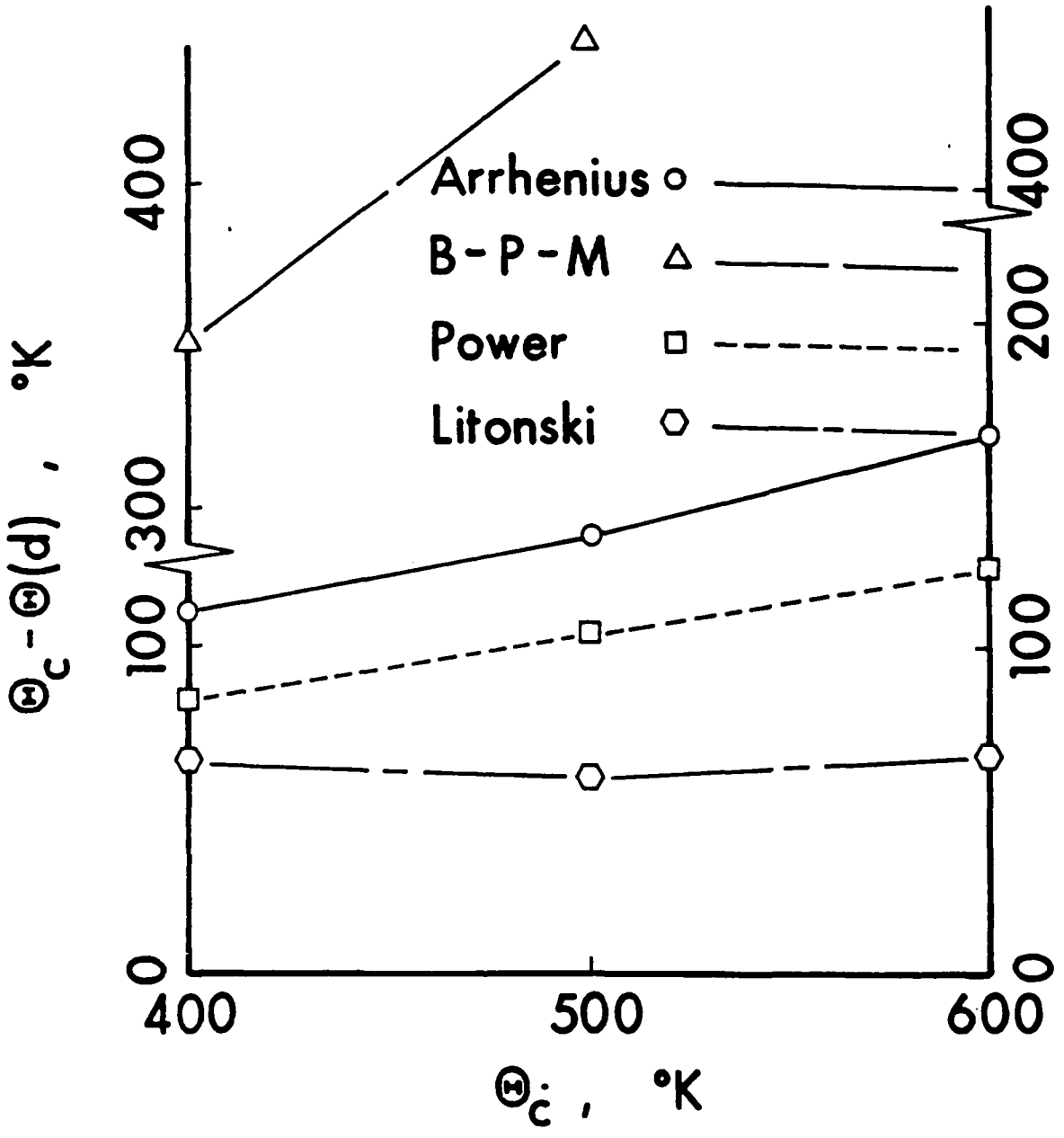

Figure 10. Temperature Contrast vs Central Temperature When the Central Plastic Strain Rate is $5 \times 10^4 s^{-1}$.

As one final comment, it should be noted that central temperatures and temperature contrasts across the band need not be large. Even for very narrow profiles, the highest temperatures achieved need be nowhere near the melting temperature for the material.

LIST OF REFERENCES

1. Wright, T. W. and Batra, R. C., "The Initiation and Growth of Adiabatic Shear Bands," Int. J. Plasticity v. 1 (1985) 205-212.

2. Wright, T. W. and Batra, R. C., "Further Results on the Initiation and Growth of Adiabatic Shear Bands at High Strain Rates," J. de Physique v. 46, Colloque C5, (1985) 323-330.

3. Malvern, L. E., "Experimental and Theoretical Approaches to Characterization of Material Behavior at High Rates of Deformation," Proc. 3rd Oxford Conference, Mechanical Properties at High Rates of Strain 1984, ed. J. Harding, 1-20, Institute of Physics, Bristol and London 1984.

4. Shawki, T. G., Clifton, R. J., and Majda, G., "Analysis of Shear Strain Localization in Thermal Visco-Plastic Materials," Brown University Report ARO DAAG29-81-K-0121/3, 1983.

5. Merzer, A. M., "Modeling of Adiabatic Shear Band Development from Small Imperfections," J. Mech. Phys. Solids, v. 30 (1983) 323-338.

6. Burns, T. J., "Approximate Linear Stability Analysis of a Model of Adiabatic Shear Formation," Quart. Appl. Math., v. 43 (1985) 65-84.

7. Moss, G. L., "Shear Strains, Strain Rates, and Temperature Changes in Adiabatic Shear Bands," 299-312 in Shock Waves and High-Strain-Rate Phenomena in Metals ed. M. A. Meyers and L. E. Murr, Plenum Press, New York 1981.

DISTRIBUTION LIST

No. of Copies	Organization
12	Administrator Defense Technical Info Center ATTN: DTIC-FDAC Cameron Station, Bldg 5 Alexandria, VA 22304-6145
4	Director Defense Advanced Research Projects Agency ATTN: Tech Info Dr. E. Van Reuth Dr. G. Faraum Dr. B. Wilcox 1400 Wilson Boulevard Arlington, VA 22209
1	Deputy Assistant Secretary of the Army (R&D) Department of the Army Washington, DC 20310
1	HQDA DAMA-ART-M Washington, DC 20310
1	C.I.A. OIR/DB/Standard GE47 HQ Washington, DC 20505
1	Commander U.S. Army War College ATTN: Lib Carlisle Barracks, PA 17013
1	Commander U.S. Army Command and General Staff College ATTN: Archives Fort Leavenworth, KS 66027
1	Commander U.S. Army Materiel Command ATTN: AMCDRA-ST 5001 Eisenhower Avenue Alexandria, VA 22333-0001
1	Commander U.S. Army Armament Research, Development and Engineering Center ATTN: SMCAR-LCA, T. Davidson Dover, NJ 07801-5001
3	Commander U.S. Army Armament Research, Development and Engineering Center ATTN: SMCAR-SC, J. D. Corrie J. Beetle E. Bloore Dover, NJ 07801-5001
1	Commander U.S. Army ARDEC ATTN: SMCAR-TDC Dover, NJ 07801
1	Commander U.S. Army Armament Research, Development and Engineering Center ATTN: SMCAR-MSI Dover, NJ 07801-5001
1	Commander Benet Weapons Laboratory ATTN: Dr. E. Schneider Watervliet, NY 12189
1	Director U.S. AMCCOM ARDEC CCAC Benet Weapons Laboratory ATTN: SMCAR-CCB-TL Watervliet, NY 12189-4050
1	Commander U.S. Army Armament, Munitions and Chemical Command ATTN: AMSMC-IMP-L Rock Island, IL 61299-7300

DISTRIBUTION LIST

No. of Copies	Organization
1	Commander U.S. Army Aviation Systems Command ATTN: AMSAV-ES 4300 Goodfellow Boulevard St. Louis, MO 63120-1798
1	Director U.S. Army Aviation Research and Technology Activity Ames Research Center Moffett Field, CA 94035-1099
1	Commander U.S. Army Communications - Electronics Command ATTN: AMSEL-ED Fort Monmouth, NJ 07703-5301
1	Commander CECOM R&D Technical Library ATTN: AMSEL-IM-L (Reports Section) B.2700 Fort Monmouth, NJ 07703-5000
1	Commander U.S. Army Harry Diamond Laboratory ATTN: SLCHD-TA-L 2800 Powder Mill Road Adelphi, MD 20783
1	Commander MICOM Research, Development and Engineering Center ATTN: AMSMI-RD Redstone Arsenal, AL 35898-5500
1	Director Missile and Space Intelligence Center ATTN: AIAM-S-YDL Redstone Arsenal, AL 35898-5500
3	Director BMD Advanced Technology Center ATTN: ATC-T, M. Capps ATC-M, S. Brockway ATC-RN, P. Boyd P.O. Box 1500 Huntsville, AL 35807
2	Commander U.S. Army Mobility Equipment Research & Development Command ATTN: DRDME-WC DRSME-RZT Fort Belvoir, VA 22060
1	Commander U.S. Army Natick Research and Development Center ATTN: DRXRE, Dr. D. Sieling Natick, MA 01762
1	Commander U.S. Army Tank Automotive Command ATTN: AMSTA-TSL Warren, MI 48397-5000
1	Commander USAG ATTN: Technical Library Fort Huachuca, AZ 85613-6000
1	Commander U.S. Army Development and Employment Agency ATTN: MODE-ORO Fort Lewis, WA 98433
3	Commander U.S. Army Laboratory Command Materials Technology Laboratory ATTN: SLCMT-T, J. Mescall SLCMT-T, R. Shea SLCMT-H, S.C. Chou Watertown, MA 02172-0001

DISTRIBUTION LIST

No. of Copies	Organization
1	Director U.S. Army TRADOC Analysis Center ATTN: ATOR-TSL White Sands Missile Range, 88002-5502
1	Commandant U.S. Army Infantry School ATTN: ATSH-CD-CS-OR Fort Benning, GA 31905-5400
1	Director U.S. Army Advanced BMD Technology Center ATTN: CRDABH-5, W. Loomis P. O. Box 1500, West Station Huntsville, AL 35807
3	Commander U.S. Army Research Office ATTN: Dr. E. Saibel Dr. G. Meyer Dr. J. Chandra P. O. Box 12211 Research Triangle Park, NC 27709
2	Commander U.S. Army Research and Standardization Group (Europe) ATTN: Dr. J. Wu Dr. F. Oertel Box 65 FPO NY 09510
3	Office of Naval Research Department of the Navy ATTN: Dr. Y. Rajapakse Dr. A. Tucker Dr. A. Kushner Washington, DC 20360
3	Commander U.S. Naval Air Systems Command ATTN: AIR-604 Washington, DC 20360
1	Commander Naval Sea Systems Command ATTN: Code SEA 62D Department of the Navy Washington, DC 20362-5101
3	Commander Naval Surface Weapons Center ATTN: Dr. W. H. Holt Dr. W. Mock Tech Lib Dahlgren, VA 22448-5000
3	Commander Naval Surface Weapons Center ATTN: Dr. R. Crowe Code R32, Dr. S. Fishman Code X211, Lib Silver Spring, MD 20902-5000
1	Commander and Director US Naval Electronics Laboratory San Diego, CA 92152
5	Air Force Armament Laboratory ATTN: AFATL/DOIL (Tech Info Center) J. Foster John Collins Joe Smith Guy Spitale Eglin AFB, FL 32542-5438
1	RADC (EMTLD, Lib) Griffiss AFB, NY 13440
1	AUL (3T-AUL-60-118) Maxwell AFB, AL 36112

DISTRIBUTION LIST

No. of Copies	Organization
1	Air Force Wright Aeronautical Laboratories Air Force Systems Command Materials Laboratory ATTN: Dr. Theodore Nicholas Wright-Patterson AFB, OH 45433
1	Air Force Wright Aeronautical Laboratories Air Force Systems Command Materials Laboratory ATTN: Dr. John P. Henderson Wright-Patterson AFB, OH 45433
1	Director Environmental Science Service Administration US Department of Commerce Boulder, CO 80302
1	Director Lawrence Livermore Laboratory ATTN: Dr. M. L. Wilkins P. O. Box 808 Livermore, CA 94550
8	Sandia National Laboratories ATTN: Dr. L. Davison Dr. P. Chen Dr. L. Bertholf Dr. W. Herrmann Dr. J. Nunziato Dr. S. Passman Dr. E. Dunn Dr. M. Forrestal P. O. Box 5800 Albuquerque, NM 87185-5800
1	Sandia National Laboratories ATTN: Dr. D. Bammann Livermore, CA 94550
1	Director National Aeronautics and Space Administration Lyndon B. Johnson Space Center ATTN: Lib Houston, TX 77058
1	Director Jet Propulsion Laboratory ATTN: Lib (TDS) 4800 Oak Grove Drive Pasadena, CA 91103
1	National Bureau of Standards ATTN: Dr. Timothy Burns Technology Building, Rm A151 Gaithersburg, MD 20899
1	A.R.A.P. Group, Titan Systems, Inc. ATTN: Ray Gogolewski 1800 Old Meadow Rd., #114 McLean, VA 22102
1	ETA Corporation ATTN: Dr. D. L. Mykkanen P. O. Box 6625 Orange, CA 92667
1	Forestal Research Center Aeronautical Engineering Lab. Princeton University ATTN: Dr. A. Eringen Princeton, NJ 08540
1	Honeywell, Inc. Defense Systems Division ATTN: Dr. Gordon Johnson 600 Second Street, NE Hopkins, MN 55343

DISTRIBUTION LIST

No. of Copies	Organization
2	Orlando Technology, Inc. ATTN: Dr. Daniel Matuska Dr. John J. Osborn P. O. Box 855 Shalimar, FL 32579
6	SRI International ATTN: Dr. Donald R. Curran Dr. Donald A. Shockey Dr. Lynn Seaman Mr. D. Erlich Dr. A. Florence Dr. R. Caligiuri 333 Ravenswood Avenue Menlo Park, CA 94025
1	Systems Planning Corporation ATTN: Mr. T. Hafer 1500 Wilson Boulevard Arlington, VA 22209
1	Terra-Tek, Inc. ATTN: Dr. Arfon Jones 420 Wakara Way University Research Park Salt Lake City, UT 84108
2	California Institute of Technology Division of Engineering and Applied Science ATTN: Dr. E. Sternberg Dr. J. Knowles Pasadena, CA 91102
1	Denver Research Institute University of Denver ATTN: Dr. R. Recht P. O. Box 10127 Denver, CO 80210
1	Massachusetts Institute of Technology ATTN: Dr. R. Probstein 77 Massachusetts Avenue Cambridge, MA 02139
1	Massachusetts Institute of Technology Department of Mechanical Engineering ATTN: Prof. L. Anand Cambridge, MA 02139
3	Rensselaer Polytechnic Institute ATTN: Prof. E. H. Lee Prof. E. Krempl Prof. J. Flaherty Troy, NY 12181
1	Southwest Research Institute Department of Mechanical Sciences ATTN: Dr. U. Lindholm 8500 Culebra Road San Antonio, TX 78228
5	Brown University Division of Engineering ATTN: Prof. R. Clifton Prof. H. Kolsky Prof. L. B. Freund Prof. A. Needleman Prof. R. Asaro Providence, RI 02912
1	Brown University Division of Applied Mathematics ATTN: Prof. C. Dafermos Providence, RI 02912
3	Carnegie-Mellon University Department of Mathematics ATTN: Dr. D. Owen Dr. M. E. Gurtin Dr. B. D. Coleman Pittsburgh, PA 15213

DISTRIBUTION LIST

No. of Copies	Organization
6	Cornell University Department of Theoretical and Applied Mechanics ATTN: Dr. Y. H. Pao Dr. A. Ruoff Dr. J. Jenkins Dr. R. Lance Dr. F. Moon Dr. E. Hart Ithaca, NY 14850
2	Harvard University Division of Engineering and Applied Physics ATTN: Prof. J. R. Rice Prof. J. Hutchinson Cambridge, MA 02138
2	Iowa State University Engineering Research Laboratory ATTN: Dr. A. Sedov Dr. G. Nariboli Ames, IA 50010
2	Lehigh University Center for the Application of Mathematics ATTN: Dr. E. Varley Dr. R. Rivlin Bethlehem, PA 18015
1	New York University Department of Mathematics ATTN: Dr. J. Keller University Heights New York, NY 10053
2	North Carolina State University Department of Civil Engineering ATTN: Prof. Y. Horie Raleigh, NC 27607
1	Pennsylvania State University Engineering Mechanical Dept. ATTN: Prof. N. Davids University Park, PA 16502
1	Rice University ATTN: Dr. C. C. Wang P. O. Box 1892 Houston, TX 77001
1	Southern Methodist University Solid Mechanics Division ATTN: Prof. H. Watson Dallas, TX 75221
1	Temple University College of Engineering Tech. ATTN: Dr. R. Haythornthwaite Dean Philadelphia, PA 19122
5	The Johns Hopkins University ATTN: Prof. R. B. Pond, Sr. Prof. R. Green Prof. W. Sharpe Prof. L. F. Bell Prof. C. A. Truesdell 34th and Charles Streets Baltimore, MD 21218
1	Tulane University Department of Mechanical Engineering ATTN: Dr. S. Cowin New Orleans, LA 70112
3	University of California Department of Mechanical Engineering ATTN: Dr. M. Carroll Dr. W. Goldsmith Dr. P. Naghdi Berkeley, CA 94[illegible]

DISTRIBUTION LIST

No. of Copies	Organization
1	University of California Dept of Aerospace and Mechanical Engineering Science ATTN: Dr. Y. C. Fung P. O. Box 109 La Jolla, CA 92037
1	University of California Department of Mechanics ATTN: Dr. R. Stern 504 Hilgard Avenue Los Angeles, CA 90024
1	University of California at Santa Barbara Department of Mechanical Engineering ATTN: Prof. T. P. Mitchel Santa Barbara, CA 93106
1	University of California at Santa Barbara Department of Materials Science ATTN: Prof. A. G. Evans Santa Barbara, CA 93106
1	University of California at San Diego Department of Mechanical Engineering ATTN: Prof. S. Nemat Nassar La Jolla, CA 92093
3	University of Delaware Department of Mechanical and Aerospace Engineering ATTN: Dr. Minoru Taya Prof. J. Vinson Newark, DE 19711
4	University of Florida Department of Engineering Science and Mechanics ATTN: Prof. L. Malvern Prof. D. Drucker Prof. E. Walsh Prof. M. Eisenberg Gainesville, FL 32601
2	University of Houston Department of Mechanical Engineering ATTN: Dr. T. Wheeler Dr. R. Nachlinger Houston, TX 77004
2	University of Illinois Department of Theoretical and Applied Mechanics ATTN: Dr. D. Carlson Prof. D. Scott Stewart Urbana, IL 61801
2	University of Illinois at Chicago Circle College of Engineering Department of Engineering, Mechanics, and Metallurgy ATTN: Prof. T.C.T. Ting Prof. D. Krajcinovic P. O. Box 4348 Chicago, IL 60680
2	University of Kentucky Department of Engineering Mechanics ATTN: Dr. M. Beatty Prof. O. Dillon, Jr. Lexington, KY 40506
1	University of Kentucky School of Engineering ATTN: Dean R. M. Bowen Lexington, KY 40506

DISTRIBUTION LIST

No. of Copies	Organization
2	University of Maryland Department of Mathematics ATTN: Prof. S. Antman Prof. T. P. Liu College Park, MD 20742
3	University of Minnesota Department of Engineering Mechanics ATTN: Prof. J. L. Erickson Prof. R. Fosdick Prof. R. James Minneapolis, MN 55455
1	University of Missouri-Rolla Department of Engineering Mechanics ATTN: Prof. R. C. Batra Rolla, MO 65401-0249
2	University of Oklahoma School of Aerospace, Mechanical and Nuclear Engineering ATTN: Prof. Akhtar S. Khan Prof. Charles W. Bert Norman, Oklahoma 73019
1	University of Pennsylvania Towne School of Civil and Mechanical Engineering ATTN: Prof. Z. Hashin Philadelphia, PA 19105
4	University of Texas Department of Engineering Mechanics ATTN: Dr. M. Stern Dr. M. Bedford Prof. Ripperger Dr. J. T. Oden Austin, TX 78712
1	University of Washington Department of Aeronautics and Astronautics ATTN: Dr. Ian M. Fyfe 206 Guggenheim Hall Seattle, WA 98195
1	University of Wyoming Department of Mathematics ATTN: Prof. R. E. Ewing P. O. Box 3036 University Station Laramie, WY 82070
3	Washington State University Department of Physics ATTN: Prof. R. Fowles Prof. G. Duvall Prof. Y. Gupta Pullman, WA 99163
2	Yale University ATTN: Dr. B.-T. Chu Dr. E. Onat 400 Temple Street New Haven, CT 96520

Aberdeen Proving Ground

Dir, USAMSAA
ATTN: AMXSY-D
AMXSY-MP, H. Cohen
Cdr, USATECOM
ATTN: AMSTE-SI-F
Cdr, CRDC, AMCCOM
ATTN: SMCCR-RSP-A
SMCCR-MU
SMCCR-SPS-IL

USER EVALUATION SHEET/CHANGE OF ADDRESS

This Laboratory undertakes a continuing effort to improve the quality of the reports it publishes. Your comments/answers to the items/questions below will aid us in our efforts.

1. BRL Report Number_____ Date of Report_____

2. Date Report Received_____

3. Does this report satisfy a need? (Comment on purpose, related project, or other area of interest for which the report will be used.)_____

4. How specifically, is the report being used? (Information source, design data, procedure, source of ideas, etc.)_____

5. Has the information in this report led to any quantitative savings as far as man-hours or dollars saved, operating costs avoided or efficiencies achieved, etc? If so, please elaborate._____

6. General Comments. What do you think should be changed to improve future reports? (Indicate changes to organization, technical content, format, etc.)

CURRENT ADDRESS

Name

Organization

Address

City, State, Zip

7. If indicating a Change of Address or Address Correction, please provide the New or Correct Address in Block 6 above and the Old or Incorrect address below.

OLD ADDRESS

Name

Organization

Address

City, State, Zip

(Remove this sheet, fold as indicated, staple or tape closed, and mail.)

FOLD HERE

Director
US Army Ballistic Research Laboratory
ATTN: DRXBR-OD-ST
Aberdeen Proving Ground, MD 21005-5066

NO POSTAGE
NECESSARY
IF MAILED
IN THE
UNITED STATES

OFFICIAL BUSINESS
PENALTY FOR PRIVATE USE, $300

BUSINESS REPLY MAIL
FIRST CLASS PERMIT NO 12062 WASHINGTON, DC
POSTAGE WILL BE PAID BY DEPARTMENT OF THE ARMY

Director
US Army Ballistic Research Laboratory
ATTN: DRXBR-OD-ST
Aberdeen Proving Ground, MD 21005-9989

FOLD HERE

END

10-87

DTIC